DOI: 10.1002/asia.200600034

Mechanism of Remote Conjugate Addition of Lithium Organocuprates to Polyconjugated Carbonyl Compounds

Naohiko Yoshikai,[a] Tatsuya Yamashita,[a] and Eiichi Nakamura*[a, b]

Abstract: Regioselective reaction of a lithium organocuprate (R_2CuLi) and a polyconjugated carbonyl compound affords a remote-conjugate-addition product. This reaction proceeds particularly cleanly when the conjugation is terminated by a C–C triple bond. The reaction pathways and the origin of the regioselectivity of this class of transformations are explored with the aid of density functional calculations. The outline of the reaction pathway is as follows. An initially formed β-cuprio-(III) enolate intermediate undergoes smooth copper migration along the conjugated system. This process takes place faster than reductive elimination of intermediary σ/π-allylcopper(III) species, since the latter reaction disrupts the conjugation in the substrate and hence is not preferred. The copper migration to the acetylenic terminal affords a σ/π-allenylcopper(III) intermediate, which undergoes facile and selective C–C bond forming reductive elimination at the terminal carbon atom. The present mechanistic framework shows good agreement with some pertinent experimental data, including ^{13}C NMR chemical shifts and kinetic isotope effects.

Keywords: conjugate addition · density functional calculations · kinetic isotope effects · organocuprates · reaction mechanisms

Introduction

Conjugate addition of a nucleophile to a Michael acceptor, in particular, an α,β-unsaturated carbonyl compound, represents one of the most fundamental organic transformations.[1] Extension of the multiple bond in the Michael acceptor can potentially result in C–C bond formation at one of the remote carbon atoms. In many cases, however, the regioselectivity may be poor, unpredictable, or condition-dependent, and the origin of the regioselectivity is often difficult to determine with certainty.[2,3] A remarkable exception in this respect is the conjugate addition of a lithium organocuprate (R_2CuLi) to polyenynyl carbonyl compounds, where the C–C bond formation takes place selectively or exclusively at the carbon atom that is most remote from the acceptor [Eq. (1)].[4]

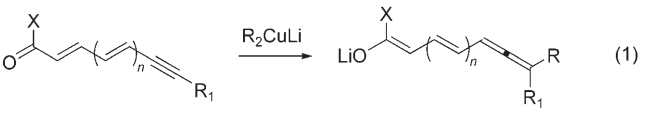

(1)

As this reaction is extremely regioselective and useful for the synthesis of allene derivatives, extensive synthetic studies have been carried out by Krause and co-workers.[4,5] The same group also reported mechanistic studies on 1,6-addition to ethyl 6,6-dimethylhept-2-en-4-ynoate, the summary of which is described as follows. First, the $^1H/^{13}C$ NMR spectroscopic analysis of the reaction with $(tBu)_2CuLi{\cdot}LiCN$ or $Me_2CuLi{\cdot}LiCN$ showed the formation of an intermediate assigned to **I**, in which the lithium and the copper atoms interact with the carbonyl oxygen and the nearby C=C double bond, respectively (Scheme 1).[6] Interestingly, no other intermediates relevant to the 1,6-addition product (such as **V**) were observed. Second, the kinetic study with $Me_2CuLi{\cdot}LiI$ showed that the reaction is first order with respect to the intermediate **I**, and that the activation energy is 70 kJ mol^{-1} (16.7 kcal mol^{-1}).[7]

[a] N. Yoshikai, T. Yamashita, E. Nakamura
Department of Chemistry, The University of Tokyo
Bunkyo-ku, Tokyo 113-0033 (Japan)
Fax: (+81) 3-5800-6889
E-mail: nakamura@chem.s.u-tokyo.ac.jp

[b] E. Nakamura
ERATO Nakamura Functional Carbon Cluster Project
Japan Science and Technology Agency
Bunkyo-ku, Tokyo 113-0033 (Japan)
E-mail: nakamura@chem.s.u-tokyo.ac.jp

Supporting information for this article is available on the WWW under http://www.chemasianj.org or from the author.

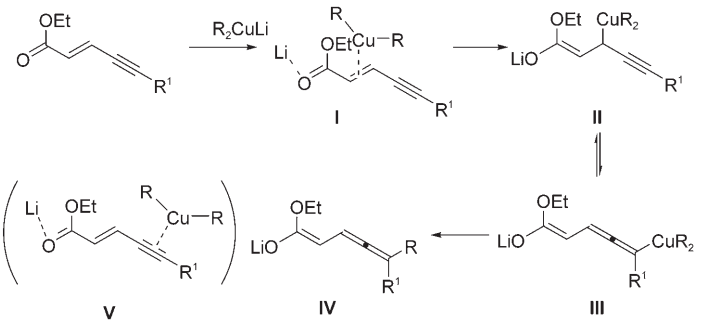

Scheme 1. A proposed mechanism for 1,6-conjugate addition of lithium organocuprate to enynoate.

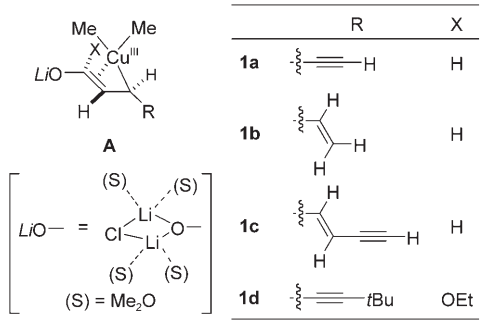

Figure 1. Chemical models of the key intermediates in the remote conjugate addition to polyconjugated carbonyl compounds.

On the basis of these experimental observations, a mechanistic scheme that involves migration of the copper atom to the acetylenic moiety and reductive elimination of the resulting organocopper(III) intermediate was proposed (Scheme 1). However, the lack of structural information except for **I** has hampered the understanding of the overall reaction pathway, the rate-determining step, and the origin of the regioselectivity.

With our long-standing interests in organocopper reaction mechanisms,[8] we have explored the reaction pathways of several relevant chemical models with the aid of density functional calculations. Concomitantly with our preliminary communication,[9] Mori, Uerdingen, Krause, and Morokuma (MUKM) reported ^{13}C kinetic isotope effects (KIEs) on the above reaction and their own theoretical study.[10] While their paper concluded that the final C–C bond formation is the rate-determining step of the reaction, we propose herein that the reported KIE can be reconciled better by a mechanism in which the copper migration is the rate-determining step.

Computational Models and Methods

We explored the reactivity of organocopper(III) complexes of a generic structure **A** in which the lithium atoms are solvated by Me_2O molecules (Figure 1, **1a–d**). Note that the β-cuprio(III) enolate such as **A** and the π complex such as **I** must be chemically equivalent to one another (see below).[8,11] Our previous studies on various model reactions showed that solvation of the lithium atoms is necessary for reproduction of the experimental parameters.[11] We therefore employed Me_2O to maintain tetracoordination of the lithium atom throughout the reaction course.

For detailed study of potential surfaces, structures, and molecular orbitals, we employed model complexes **1a–c**, derived from pent-2-en-4-ynal, penta-2,4-dienal, and hepta-2,4-dien-6-ynal, respectively. For these models, we examined all possible reaction pathways: 1,4- and 1,6-additions for **1a** and **1b**, and 1,4-, 1,6-, and 1,8-additions for **1c**. For comparison with the experimental data for the 1,6-addition to ethyl 6,6-dimethylhept-2-en-4-ynoate,[6,7] we employed a more realistic model **1d**.

All calculations were performed with a Gaussian 03 package.[12] Density functional theory (DFT) was employed by using the B3LYP hybrid functional.[13] Structures were optimized with a basis set consisting of the Stuttgart–Dresden effective core potential (SDD) for Cu[14] and 6-31G(d) or 3-21G[15] for the rest (denoted as 631SDD and 321SDD, respectively). The two basis sets gave similar structures; for example, the differences in bond lengths are less than 0.1 Å. For B3LYP/321SDD-optimized structures, single-point energy calculations were performed at the B3LYP/631SDD level, which gave similar energetics as the B3LYP/631SDD optimization; the relative energies obtained by the two methods are within 1 kcal mol^{-1} (for most cases 0.5 kcal mol^{-1}) apart. The method and basis sets used here have been applied to 1,4-conjugate addition and related reactions of lithium organocuprates and are known to give reliable results.[11,16] Each stationary point was adequately characterized by normal coordinate analysis. The intrinsic reaction coordinate (IRC) analysis[17] was carried out at the B3LYP/321SDD level to confirm that the stationary points are smoothly connected to each other. For NMR chemical shift calculations, the gauge-independent atomic orbital (GIAO) method[18] was employed in single-point calculations at the B3LYP/6311+SDD (SDD for Cu and 6-311+G(d) for the rest) level on structures optimized at the B3LYP/321SDD level. KIEs were calculated by the Bigeleisen–Mayer equation with Wigner tunneling correction,[19] using frequencies corrected by 0.9614.[20] Localized Kohn–Sham orbitals were obtained by the Boys localization procedure.[21]

Abstract in Japanese:

リチウムクプラート（R_2CuLi）とポリ共役カルボニル化合物の反応は，共役末端に炭素炭素三重結合がある場合特に高い位置選択性で遠隔共役付加生成物を与える．本反応の機構及び位置選択性の由来について密度汎関数計算により検討を行った．反応経路の概要は以下の通りである：始めに生成するβ-クプリオ(III)エノラート錯体から，銅原子が共役鎖上を円滑に転位し，最終的にアルキン末端へ移ることによりσ/π-アレニル銅(III)中間体が生成する．この錯体が共役鎖末端の炭素原子上で速やかに還元的脱離を起こし，生成物を与える．共役鎖内部での還元的脱離は，共役系を切断するためエネルギー的に不利である．得られた計算結果は，^{13}C NMR の化学シフト値や速度論的同位体効果などの実験値とよく一致した．

Results and Discussion

Reaction Pathway of Model Systems

1,6-Addition to Pent-2-en-4-ynal

We first investigated 1,4- and 1,6-addition to pent-2-en-4-ynal starting from the model complex **1a**. Scheme 2 and Figure 2 present the reaction pathway and the energy diagram, respectively. Both **2a** and **4a** give the same 1,4-adduct upon quenching of the reaction with protons, while **5a** gives the 1,6-adduct. The energy diagram immediately suggests that the kinetically and thermodynamically most favorable pathway is the 1,6-addition pathway through an organocopper(III) intermediate **3a**. Migration of the copper atom (**1a**→**3a**) and reductive elimination of **3a** at the C6 atom via **TS4a** gives the 1,6-adduct; copper migration is the rate-determining step in this case. Reductive elimination of **1a** and **3a** at the C4 atom (via **TS1a** and **TS3a**) to give the 1,4-adduct is kinetically less favorable than the 1,6-addition. Remarkably, the 1,6-reductive elimination of **3a** requires a much lower activation energy than the 1,4-reductive elimination of **1a**. This will be discussed in detail below.

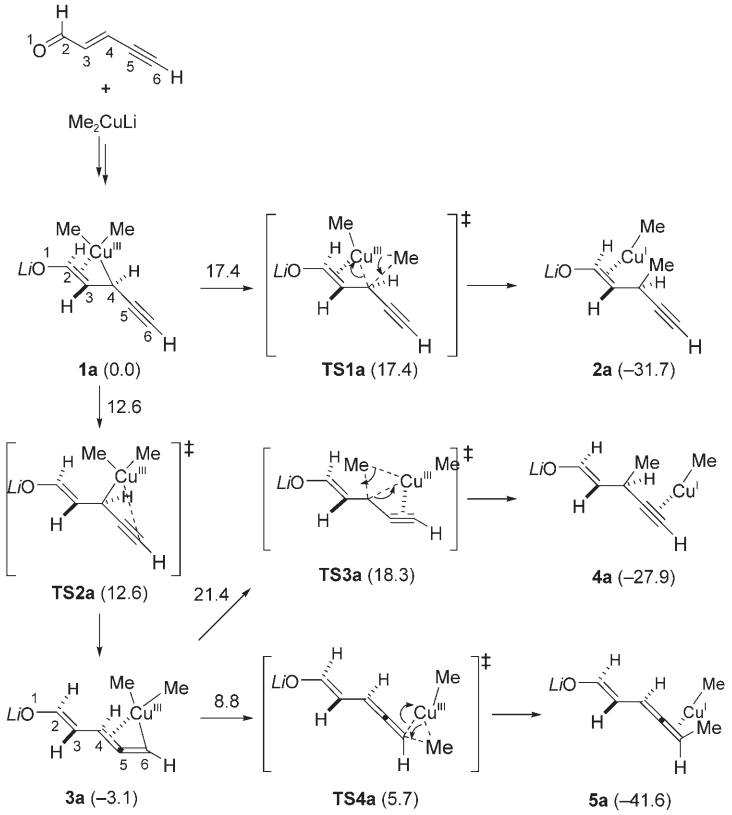

Scheme 2. Reaction pathways and potential-energy changes for 1,4- and 1,6-addition of Me_2CuLi to pent-2-en-4-ynal. Potential energies (kcal mol^{-1}, calculated at the B3LYP/631SDD level) relative to **1a** are shown in parentheses. Energy changes are shown together with arrows.

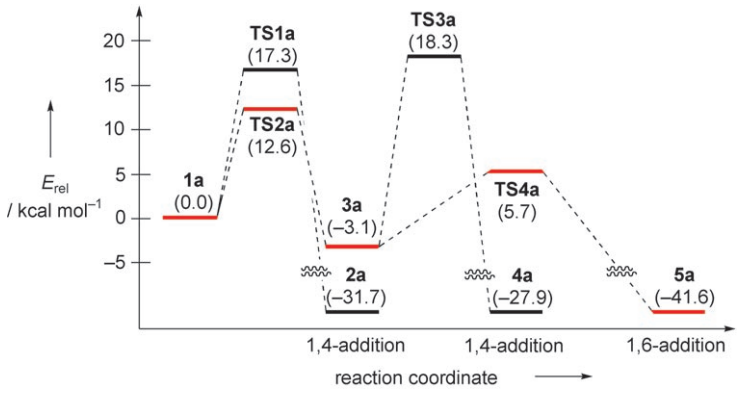

Figure 2. Potential-energy profiles for 1,4- and 1,6-addition to pent-2-en-4-ynal (B3LYP/631SDD). The energetically favored 1,6-pathway is shown in red.

The first intermediate **1a** has a structure that is essentially the same as that formed in the 1,4-conjugate addition of Me_2CuLi to an α,β-unsaturated carbonyl compound (Figure 3),[8,11] and it can undergo reductive elimination via **TS1a** to give the 1,4-addition product **2a**. The activation energy (17.3 kcal mol^{-1}) is higher than that of simple 1,4-addition to an acrolein or a cyclohexenone molecule (≈12–15 kcal mol^{-1}),[8,11] because the C–C bond formation disturbs the enyne conjugation system present in **1a**.[22]

Alternatively, the Me_2Cu moiety in **1a** can migrate to the C5–C6 triple bond (via **TS2a**) to form a new organocopper(III) intermediate **3a. TS2a** contains an intrinsically unstable T-shaped triorganocopper(III) geometry (Figure 3).[23] While a related process, π→σ isomerization of allyldimethylcopper(III), requires an activation energy as much as 19 kcal mol^{-1},[22] this copper migration is kinetically much more facile ($\Delta E^{\neq}$ = 12.6 kcal mol^{-1}) and is thus preferred over the C–C bond formation via **TS1a** by 4.7 kcal mol^{-1}. The low activation energy of the copper migration can be ascribed to coordination of the terminal acetylene moiety in **TS2a** (Figure 3), judging from the moderately short Cu–C5 distance (2.335 Å) and bending of the C4–C6 acetylenic moiety (167.3°).

The intermediate **3a** has a distorted square-planar geometry, in which the copper atom is much more strongly bonded to the terminal C6 atom (Cu–C6: 1.977 Å) than to the C4 atom (Cu–C4: 2.556 Å) (Figure 3). This structural feature indicates that the copper atom is σ-bonded to the C6 atom and π-coordinated by the C4–C5 bond, and hence **3a** may be called a σ/π-allenylcopper(III) complex.[22,24] Localized Kohn–Sham orbitals of **3a** also confirm this conjecture (Figure 4). The dissymmetric bonding would be the result of the intrinsic stability of a C(sp^2)–metal bond (relative to a C(sp^3)–metal bond) and the electron-rich enolate substituent at the C4 atom.[22]

The complex **3a** can undergo reductive elimination either at the C4 atom via **TS3a** or at the C6 atom via **TS4a** (Scheme 2); the latter pathway to the 1,6-adduct **5a** ($\Delta E^{\neq}$ = 8.8 kcal mol^{-1}) is kinetically much more favorable than the former to the 1,4-adduct **4a** ($\Delta E^{\neq}$ = 21.4 kcal mol^{-1}). The high activation energy for the former pathway is partially due to the disruption of the C2–C5 conjugation (see above). The dissymmetric bonding of **3a** also indicates that the

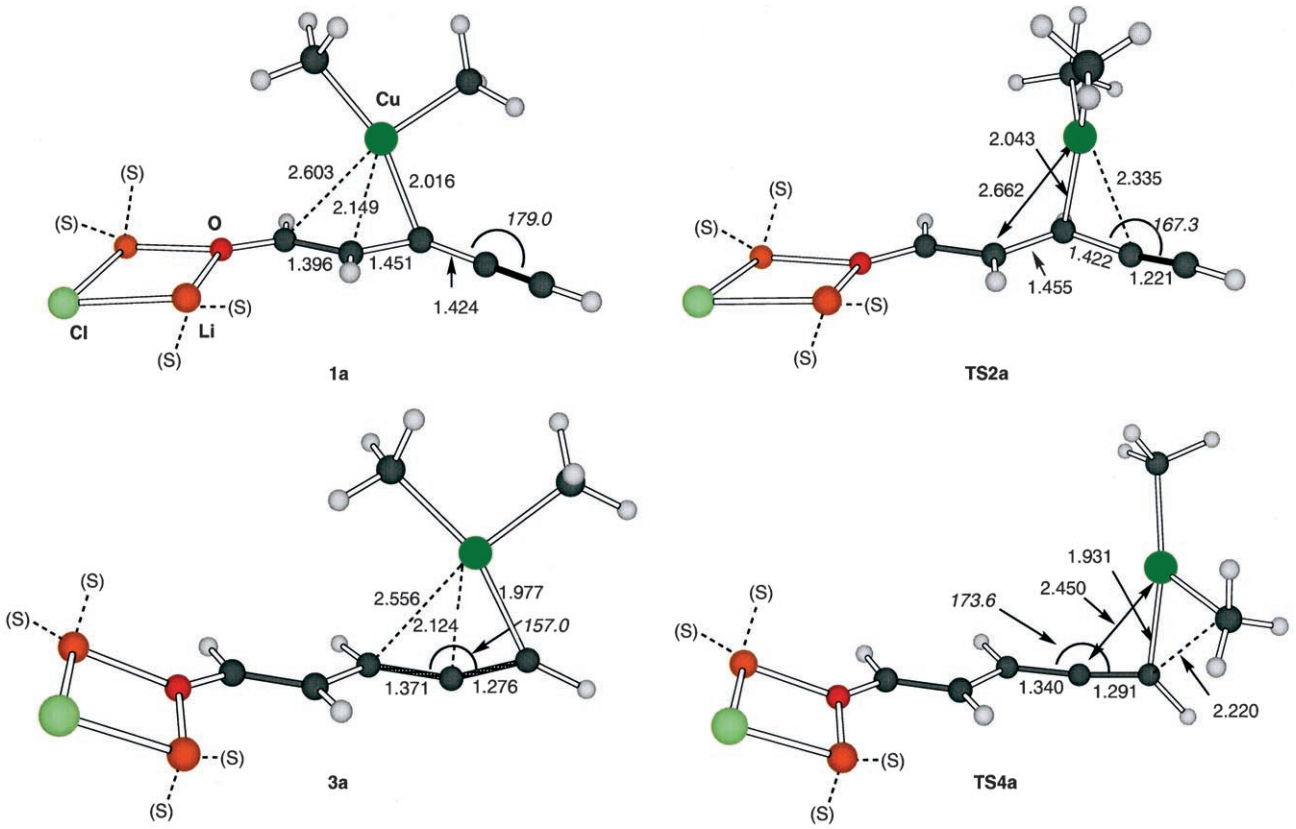

Figure 3. Structures of the intermediates and the transition states involved in 1,6-addition of Me_2CuLi to pent-2-en-4-ynal (B3LYP/631SDD). (S) represents a Me_2O molecule coordinated to a lithium atom. The values refer to bond lengths (Å) and bond angles (degrees, italics).

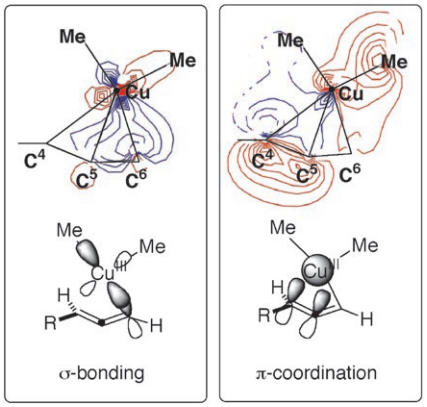

Figure 4. Localized Kohn–Sham orbitals (contour maps and their schematic representations) of σ/π-allenylcopper(III) intermediate **3a** (B3LYP/631SDD). Left: σ-bonding between Cu and C6; right: π-coordination from C4=C5 to Cu.

copper(III) atom cannot effectively recover its d electrons by reductive elimination at the π-coordinated C4 terminal.[22] The activation energy for the 1,6-adduct formation is remarkably low relative to those for reductive elimination of structurally related organocopper(III) complexes (e.g. β-cuprio(III) enolate and π-allylcopper(III)).[11,22] This must be due to strain release into the intrinsically linear allene: to release the strain of the C4–C5–C6 bond (from 157.0° to 173.6°), the C4–C5 double bond of **3a** becomes detached from the copper(III) center. This gives a kinetically unstable triorganocopper(III) species,[23] which then undergoes rapid reductive elimination. Participation of the allenyl C5–C6 π orbital that is orthogonal to the Cu–C6 σ bond in C–C bond formation may also contribute to the low activation barrier.[25]

1,6-Addition to Penta-2,4-dienal

Next, 1,4- and 1,6-addition to penta-2,4-dienal were investigated, starting from the complex **1b**. Such a reaction often gives a mixture of 1,4- and 1,6-adducts depending on the specific reaction conditions.[2] Scheme 3 and Figure 5 show the reaction pathway and the energy profile, respectively. As with pent-2-en-4-ynal, the kinetically most favorable pathway involves copper migration to the C5–C6 double bond (**1b**→**3b**; $\Delta E^{\ddagger} = 16.2$ kcal mol^{-1}) and subsequent reductive elimination at the C6 terminal (**3b**→**5b**; $\Delta E^{\ddagger} = 13.5$ kcal mol^{-1}). The activation barriers of the 1,4- and 1,6-addition pathways are closer to each other than in the enyne system (Figures 2 and 5).

Although the rate-determining step in this case is again the migration of the copper atom, the activation energy is higher than that of the enyne system (Figure 2: **1a**→**3a**; $\Delta E^{\ddagger} = 12.6$ kcal mol^{-1}). This is probably due to the weaker interaction between the migrating Cu^{III} atom and the C5–

C6 multiple bond in **TS2b** than in **TS2a**. The longer Cu–C5 distance in **TS2b** (2.432 Å) than in **TS2a** (2.335 Å) supports this conjecture (Figures 3 and 6).

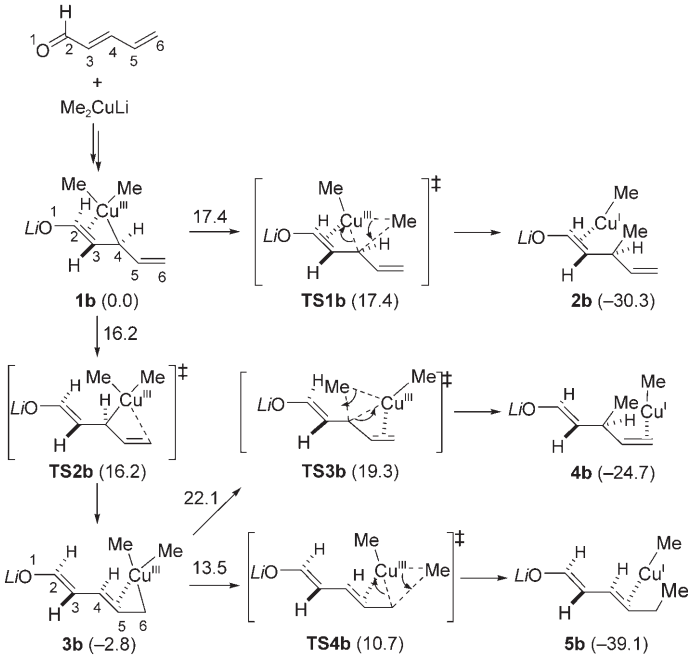

Scheme 3. Reaction pathways and potential-energy changes for 1,4- and 1,6-addition of Me_2CuLi to penta-2,4-dienal (B3LYP/631SDD). Potential energies (kcal mol^{-1}) relative to **1b** are shown in parentheses. Energy changes are shown together with arrows.

The reductive elimination at the olefin terminal via an enyl [σ+π]-type transition state (TS) (**TS5b**) requires an activation energy of 13.5 kcal mol^{-1}, which is comparable to that of 1,4-conjugate addition to acrolein or cyclohexenone, but much higher than that of 1,6-reductive elimination at the acetylene terminal (**TS5a**, 8.8 kcal mol^{-1}). This implies that the regioselectivity of remote conjugate addition may be lower for polyene systems than for polyenyne systems.

1,8-Addition to Hepta-2,4-dien-6-ynal

Next, we investigated 1,4-, 1,6- and 1,8-additions to a more-extended substrate, hepta-2,4-dien-6-ynal. Scheme 4 and

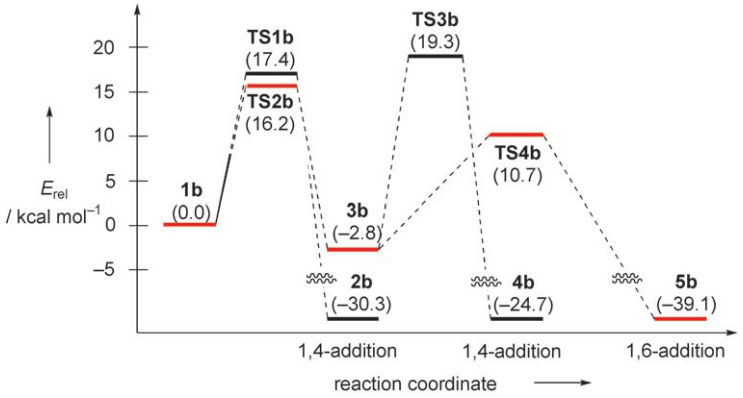

Figure 5. Potential-energy profiles for 1,4- and 1,6-addition to penta-2,4-dienal (B3LYP/631SDD). The energetically favored 1,6-pathway is shown in red.

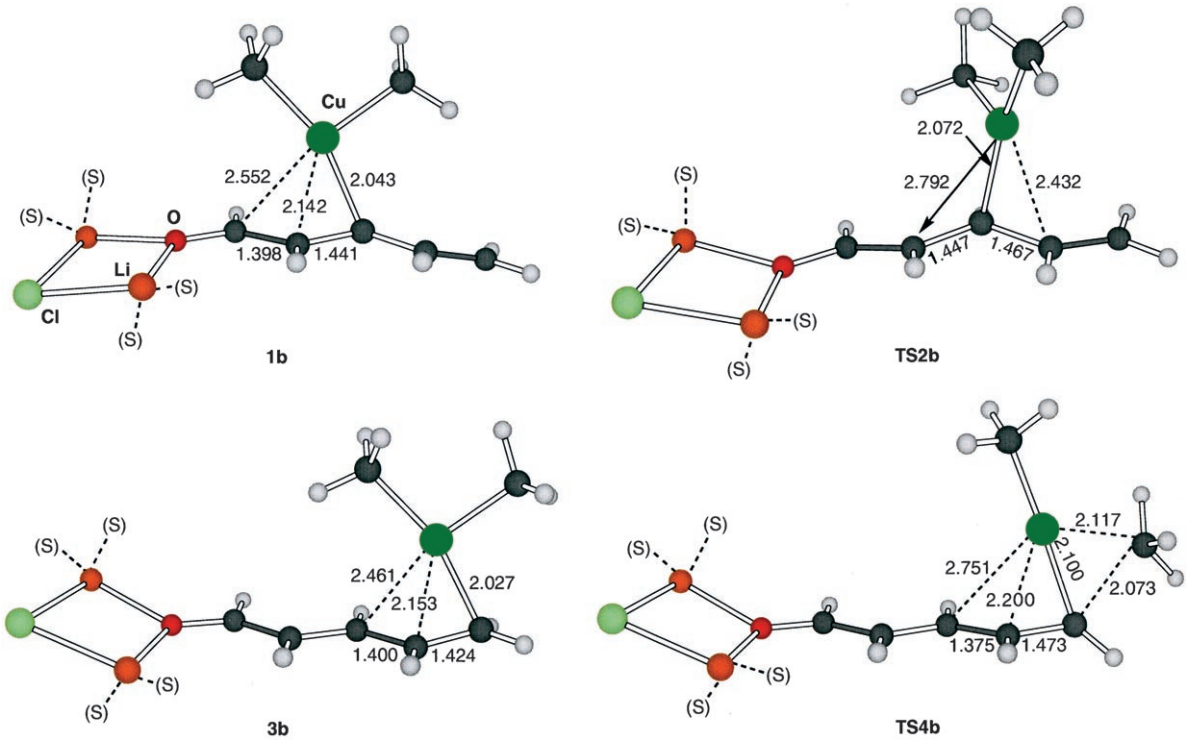

Figure 6. Structures of the intermediates and the transition states involved in 1,6-addition of Me_2CuLi to penta-2,4-dienal (B3LYP/631SDD). (S) represents a Me_2O molecule coordinated to a lithium atom. The values refer to bond lengths (Å) and bond angles (degrees, italics).

CHEMISTRY
AN ASIAN JOURNAL

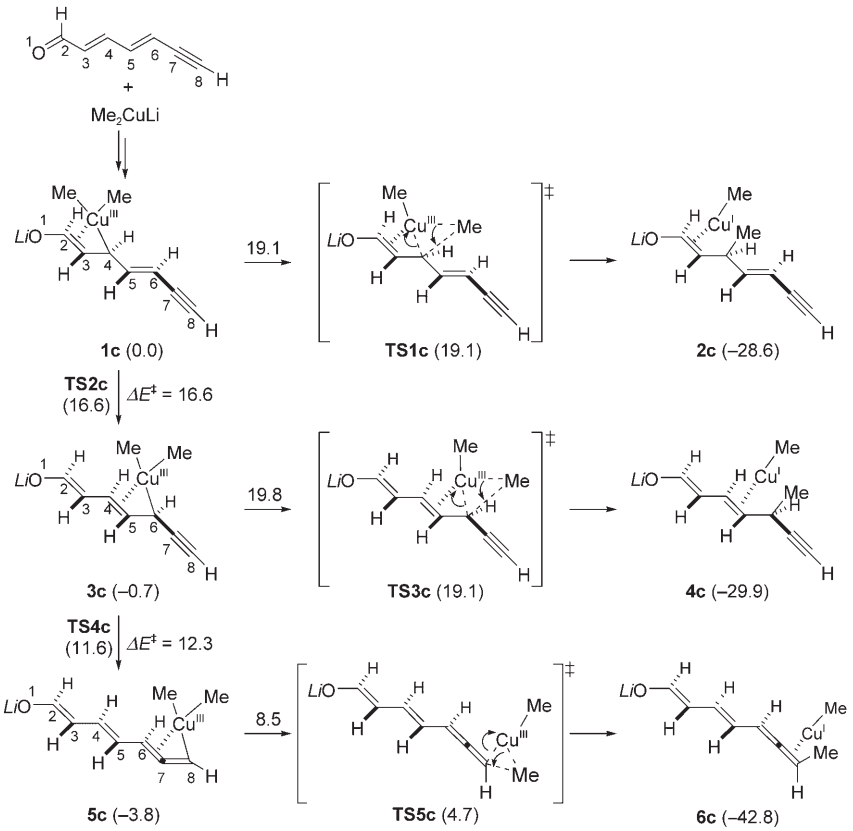

Scheme 4. Reaction pathways and potential-energy changes for 1,4-, 1,6- and 1,8-addition of Me_2CuLi to hepta-2,4-dien-6-ynal (B3LYP/631SDD). Potential energies (kcal mol^{-1}) relative to **1c** are shown in parentheses. Energy changes are shown together with arrows.

Figure 7 show the reaction pathways and the energy profiles, respectively.[26] In accordance with the experiments, the 1,8-addition pathway is kinetically the most favorable. This reaction involves migration of the copper atom (**1c**→**3c**→**5c**) and reductive elimination of the resulting σ/π-allenylcopper(III) complex **5c** at the acetylene terminal. The rate-determining step is the first copper migration, which requires higher activation energy (16.6 kcal mol^{-1}) than the second one (12.3 kcal mol^{-1}) due to weaker stabilization of the copper(III) center in **TS2c** than in **TS4c** (see above). As with the shorter homologues, reductive elimination at the internal carbon atoms of **1c**, **3c**, and **5c**, which give 1,4- or 1,6-adducts, is kinetically much less favorable due to disruption of the conjugation of the substrate.[26]

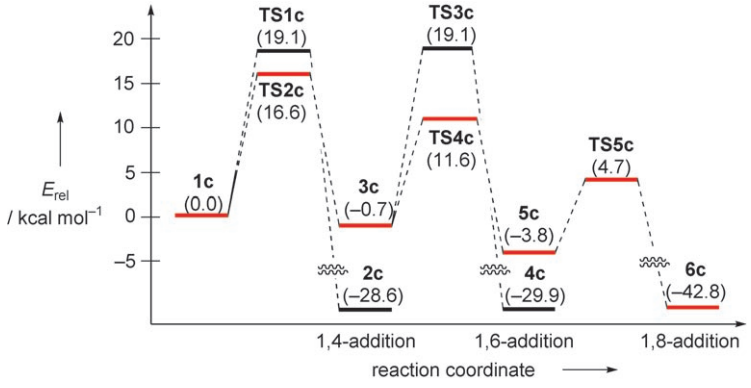

Figure 7. Potential-energy profiles for 1,4-, 1,6-, and 1,8-addition pathways (B3LYP/631SDD). The energetically favored 1,8-pathway is shown in red.

Reaction Pathway of a Realistic System

1,6-Addition to Ethyl 6,6-Dimethylhept-2-en-4-ynoate

We investigated the structure and the reaction pathway of the model complex **1d** for comparison with the experimental results of Krause and co-workers. First, we calculated the ^{13}C NMR chemical shift values of ethyl 6,6-dimethylhept-2-en-4-ynoate and its copper complex **1d** after geometry optimization. Figure 8 shows the comparison of experimental and computational results.[6]

The downfield shift of the C1 signal and the upfield shift of the C2 and C3 signals observed in the experiments are ascribed to coordination of the carbonyl oxygen to the lithium atom and back-donation from the copper atom to the C2–C3 double bond, respectively. Although the calculated chemical shift values of both the substrate and **1d** appeared systematically downfield by 5–10 ppm relative to the experimental values, they showed good agreement with each other with respect to their relative chemical shift values among the three carbon atoms. Furthermore, the calculation reproduced well the chemical shift change upon formation of the complex. These data support the model complex **1d** as a good representation of reality.

Figure 9 shows the reaction pathway and the energy profile of the 1,6-addition reaction. Initial copper migration (**1d**→**2d**) takes place with an activation energy of 11.9 kcal mol^{-1}, which is comparable to that of the related model system **1a** (12.6 kcal mol^{-1}; see Figure 2). On the other hand, reductive elimination of the resulting σ/π-allenylcopper(III) complex **2d** requires higher activation energy (14.0 kcal mol^{-1}) than that of the related complexes **3a** and **5c** (8.8 and 8.5 kcal mol^{-1}, respectively; see Figures 2 and 7). This would be due to steric hindrance of the *t*Bu group on the terminal carbon atom. However, the 2.1 kcal mol^{-1} difference between **TS1d** and **TS2d** is too small to be conclusive

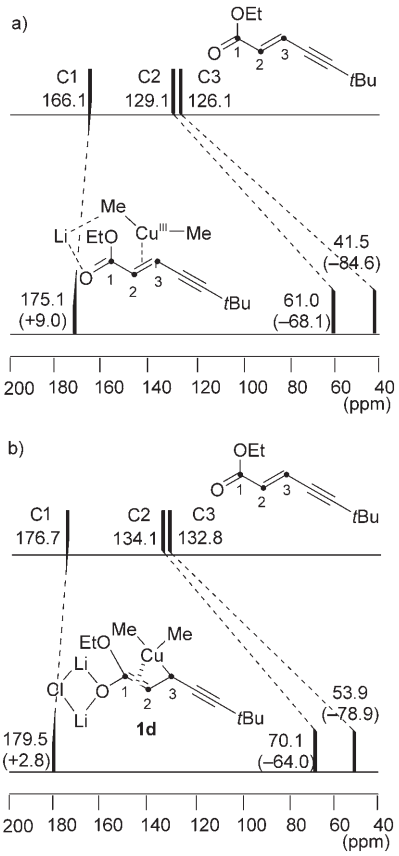

Figure 8. ^{13}C NMR chemical shift values (ppm) of ethyl 6,6-dimethylhept-2-en-4-ynoate and its complex with Me_2CuLi. a) Experiments;[6c] b) calculations (B3LYP/6311+SDD//B3LYP/321SDD). The values in parentheses refer to changes in ^{13}C NMR chemical shifts (ppm).

for the rate-determining step.[27] KIEs were therefore examined.

Measurement of KIE is a powerful experimental tool to study the nature of the rate-determining step.[28] In combination with high-level quantum chemical calculations, it provides valuable mechanistic insight into synthetic reactions, including organocuprate reactions.[29,30] From a computational point of view, KIE would be a better measure than energy for comparison with experiments, as molecular structures, which are closely related to frequencies and thus to KIE, are much less susceptible to the computational methods and basis sets than energies. MUKM determined the ^{13}C KIE data for 1,6-addition of $Bu_2CuLi{\cdot}LiCN$ to ethyl 6,6-dimethylhept-2-en-4-ynoate, performed calculations with an organocuprate model EtMeCuLi·LiCl (incoming group = Et), and concluded that the C–C bond formation is the rate-determining step ([Eq. (2)] and Table 1, second and third column).[10]

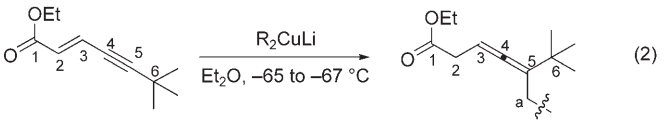

We saw problems in this conclusion. Looking into the experimental data of MUKM, one may find that the KIE (1.002–1.009) on the carbon atom bonded to copper (C_a) is too small for the one participating in the rate-determining C–C bond formation. For example, the 1,4-addition of Bu_2CuLi to cyclohexenone, where the C–C bond formation is the rate-determining step, exhibits a KIE value of 1.011–1.016 on this C_a atom.[30a] Thus, a rational conclusion drawn from the experimental data would be that C–C bond formation is not the rate-determining step of the 1,6-addition reaction. In fact, the calculated KIE (1.024) on the C_a atom based on the C–C bond-forming TS appears to be unreasonably larger than these experimental data. While the theoretical level of the computation (B3LYP/Ahlrichs SVP for Cu, 6-31G(d) for the rest) is similar to ours, it did not consider coordination of solvent molecules (such as Me_2O in the present case) to lithium atoms, which affects significantly the structures and energetics of organocuprate reactions.[11] In fact, the interaction between the alkyl group and the lithium atom is rather strong in the absence of solvent molecules, which is an unlikely scenario in the light of the reaction conditions.

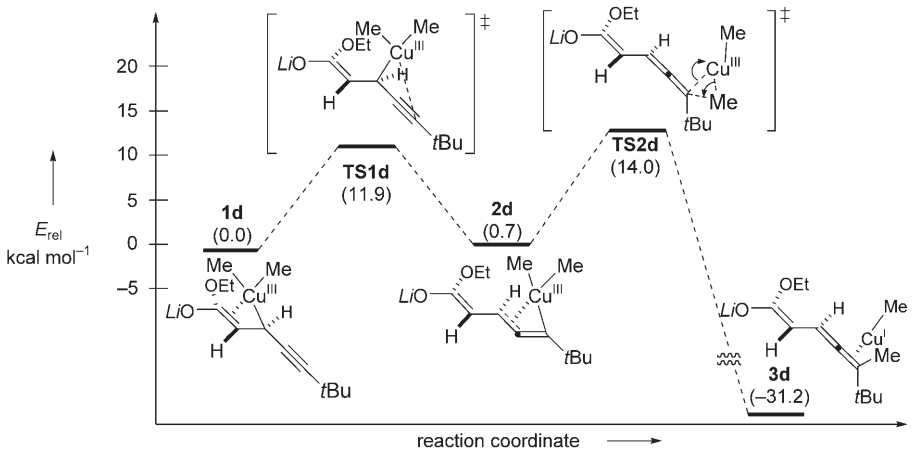

Figure 9. Reaction pathway and energy diagram for 1,6-addition of Me_2CuLi to ethyl 6,6-dimethylhept-2-en-4-ynoate (B3LYP/631SDD).

We reinvestigated the computational KIE values with our own chemical model (Table 1, fourth to seventh columns). The KIE values calculated for the copper migration step (**1d**→**TS1d**) show good to excellent agreement with experiment; the error was within ±0.005 for every carbon atom (see columns 4 and 5). The calculated KIE on the C_a atom (1.008), the most important factor in the present case, falls within the experimental data (1.002–

Table 1. Experimental and calculated $^{12}C/^{13}C$ KIE values for 1,6-addition to ethyl 6,6-dimethyl-hept-2-en-4-ynoate.

Atom	MUKM[10] experimental[a]	MUKM[10] calcd[b]	**TS1d** calcd[c]	**TS1d** calcd[d]	**TS2d** calcd[c]	**TS2d** calcd[d]
C1	1.001–1.002	1.002	1.002	1.000	1.002	0.998
C2	1.001–1.003	1.000	1.003	0.999	0.998	0.996
C3	1.001–1.003	0.998	1.000	1.002	0.988	0.988
C4	1.005–1.009	1.002	1.005	1.010	1.008	1.014
C5	1.011–1.013	1.016	1.007	1.017	1.015	1.022
C6	1.000	1.000	1.000	1.000	1.000	1.000
C_a	1.002–1.009	1.024	1.008	1.010	1.029	1.030

[a] $Bu_2CuLi{\cdot}LiCN$ ($Bu = C_aH_2CH_2CH_2CH_3$) was employed in the experiments. The C6 atom was taken as an internal standard. [b] $EtMeCuLi{\cdot}LiCl$ ($Et = C_aH_2CH_3$; without solvation to Li) was employed in the computational model. Calculation was carried out by the B3LYP method with basis sets that consist of Ahlrichs SVP (for Cu) and 6-31G(d) (for the rest). [c] Calculated at the B3LYP/321SDD level. [d] Calculated at the B3LYP/631SDD level.

1.009). On the other hand, the KIE values for the C–C bond formation (**1d**→**TS2d**) are much different: larger KIEs are obtained for the C_a, C4, and C5 atoms (column 6 and 7). Expectedly, the KIE on the C_a atom (1.029) is much larger than in the experimental data. The negative KIE on the C3 atom (0.988) also considerably deviates from the experimental data (1.001–1.003). This likely reflects the change in its hybridization (sp^3 in the reactant **1d**, sp^2 in **TS2d**). On the basis of our own KIE calculations, we conclude that the copper migration is the rate-determining step of the 1,6-addition reaction in question.

Conclusions

In summary, we propose a general mechanistic framework for remote conjugate addition of an organocuprate to a polyenynyl carbonyl compound (Scheme 5). Interaction between the substrate and the cuprate initially generates a β-cuprio(III) enolate intermediate **A**, which undergoes sequential copper migration via σ/π-allylcopper(III) intermediates. When the conjugation is terminated by an acetylenic group, the final migration gives the crucial, strained σ/π-allenylcopper(III) intermediate **B**, the kinetic instability of which results in rapid C–C bond formation at the terminal carbon atom. C–C bond formation at the internal carbon atoms is generally disfavored as it disturbs the conjugation system.

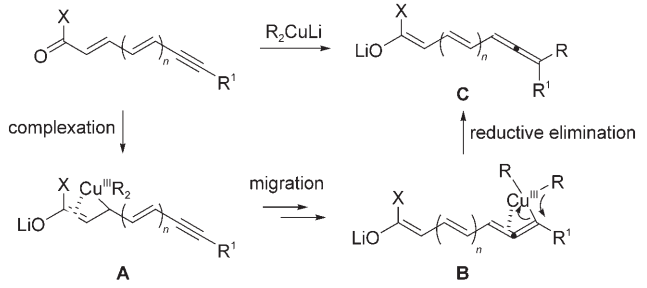

Scheme 5. A general mechanism for remote conjugate addition of lithium organocuprate to polyenyne-substituted carbonyl compounds.

The present study also explains why the regioselectivity of conjugate addition to polyenyl carbonyl compounds tends to be less reliable. Unlike those in the enyne reaction, the copper intermediates formed from a polyene substrate such as **3b** lack a decisive structural feature and may undergo C–C bond formation at any possible carbon atom depending on substrates and reaction conditions.[2]

The present and previous studies on the Lewis acid effect on the reactivity of an organocopper(III) complex provide insight into experimental observations that are confusing.[23c] For example, the contrasting selectivities of Bu_2CuLi and $BuCu{\cdot}BF_3$ (Yamamoto reagent) in the reaction with methyl sorbate may be rationalized as follows [Eq. (3)].[31] Whereas Bu_2CuLi follows our general rule of remote addition, BF_3 accelerates decomposition of the initial copper(III) intermediate so that it undergoes C–C bond formation immediately (i.e. to give the 1,4-adduct).

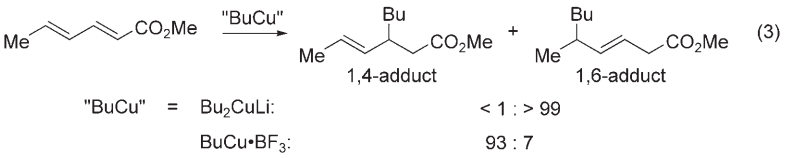

Acknowledgements

We thank the Ministry of Education, Culture, Sports, Science, and Technology of Japan for financial support and for the 21st Century COE Program for Frontiers in Fundamental Chemistry. The Research Center for Computational Science, Okazaki National Research Institute, and the Intelligent Modeling Laboratory, The University of Tokyo, are gratefully acknowledged for generous allotment of computational time.

[1] a) *Comprehensive Organic Synthesis, Vol. 3* (Eds.: B. M. Trost, I. Fleming), Pergamon Press, New York, **1991**, pp. 1–268; b) P. Perlmutter, *Conjugate Addition Reactions in Organic Synthesis*, Pergamon Press, New York, **1992**.

[2] a) J. A. Marshall, R. A. Ruden, L. K. Hirsch, M. Phillippe, *Tetrahedron Lett.* **1971**, *12*, 3795–3798; b) E. J. Corey, N. W. Boaz, *Tetrahedron Lett.* **1985**, *26*, 6019–6022; c) H. Wild, L. Born, *Angew. Chem.* **1991**, *103*, 1729; *Angew. Chem. Int. Ed. Engl.* **1991**, *30*, 1685–1687.

[3] Examples other than organocuprate addition: a) M. P. Cooke, R. J. Goswami, *J. Am. Chem. Soc.* **1977**, *99*, 642–644; b) P. Magunus, T. Gallagher, J. Schultz, Y-S. Or, T. P. Ananthanarayan, *J. Am. Chem. Soc.* **1987**, *109*, 2706–2711.

[4] a) N. Krause, A. Hoffmann-Röder in *Modern Organocopper Chemistry* (Ed.: N. Krause), Wiley-VCH, Weinheim, **2001**, pp. 145–166; b) N. Krause, A. Gerold, *Angew. Chem.* **1997**, *109*, 194–213; *Angew. Chem. Int. Ed. Engl.* **1997**, *36*, 186–204; c) N. Krause, S. Thorand, *Inorg. Chim. Acta* **1999**, *296*, 1–11, and references cited therein.

[5] A. Hoffmann-Röder, N. Krause in *Modern Allene Chemistry* (Eds.: N. Krause, A. S. H. Hashmi), Wiley-VCH, Weinheim, **2004**, pp. 51–92.

[6] a) N. Krause, *J. Org. Chem.* **1992**, *57*, 3509–3512; b) N. Krause, R. Wagner, A. Gerold, *J. Am. Chem. Soc.* **1994**, *116*, 381–382; c) J. Canisius, T. A. Mobley, S. Berger, N. Krause, *Chem. Eur. J.* **2001**, *7*, 2671–2675.
[7] J. Canisius, A. Gerold, N. Krause, *Angew. Chem.* **1999**, *111*, 1727–1730; *Angew. Chem. Int. Ed.* **1999**, *38*, 1644–1646.
[8] a) E, Nakamura, S. Mori, *Angew. Chem.* **2000**, *112*, 3902–3924; *Angew. Chem. Int. Ed.* **2000**, *39*, 3750–3771; b) E. Nakamura, S. Mori, in *Modern Organocopper Chemistry* (Ed.: N. Krause), Wiley-VCH, Weinheim, **2001**, pp. 315–346.
[9] N. Yoshikai, T. Yamashita, E. Nakamura, *Angew. Chem.* **2005**, *117*, 4799–4801; *Angew. Chem. Int. Ed.* **2005**, *44*, 4721–4723.
[10] S. Mori, M. Uerdingen, N. Krause, K. Morokuma, *Angew. Chem.* **2005**, *117*, 4795–4798; *Angew. Chem. Int. Ed.* **2005**, *44*, 4715–4720.
[11] M. Yamanaka, E. Nakamura, *Organometallics* **2001**, *20*, 5675–5681.
[12] Gaussian 03 (Revision C.02), M. J. Frisch, G. W. Trucks, H. B. Schlegel, G. E. Scuseria, M. A. Robb, J. R. Cheeseman, J. A. Montgomery, Jr., T. Vreven, K. N. Kudin, J. C. Burant, J. M. Millam, S. S. Iyengar, J. Tomasi, V. Barone, B. Mennucci, M. Cossi, G. Scalmani, N. Rega, G. A. Petersson, H. Nakatsuji, M. Hada, M. Ehara, K. Toyota, R. Fukuda, J. Hasegawa, M. Ishida, T. Nakajima, Y. Honda, O. Kitao, H. Nakai, M. Klene, X. Li, J. E. Knox, H. P. Hratchian, J. B. Cross, C. Adamo, J. Jaramillo, R. Gomperts, R. E. Stratmann, O. Yazyev, A. J. Austin, R. Cammi, C. Pomelli, J. W. Ochterski, P. Y. Ayala, K. Morokuma, G. A. Voth, P. Salvador, J. J. Dannenberg, V. G. Zakrzewski, S. Dapprich, A. D. Daniels, M. C. Strain, O. Farkas, D. K. Malick, A. D. Rabuck, K. Raghavachari, J. B. Foresman, J. V. Ortiz, Q. Cui, A. G. Baboul, S. Clifford, J. Cioslowski, B. B. Stefanov, G. Liu, A. Liashenko, P. Piskorz, I. Komaromi, R. L. Martin, D. J. Fox, T. Keith, M. A. Al-Laham, C. Y. Peng, A. Nanayakkara, M. Challacombe, P. M. W. Gill, B. Johnson, W. Chen, M. W. Wong, C. Gonzalez, J. A. Pople, Gaussian, Inc., Wallingford, **2004**.
[13] a) A. D. Becke, *J. Chem. Phys.* **1993**, *98*, 5648–5652; b) C. Lee, W. Yang, R. G. Parr, *Phys. Rev. B* **1988**, *37*, 785–789.
[14] M. Dolg, U. Wedig, H. Stoll, H. Preuss, *J. Chem. Phys.* **1987**, *86*, 866–872.
[15] W. J. Hehre, L. Radom, P. v. R. Schleyer, J. A. Pople, *Ab Initio Molecular Orbital Theory*, Wiley, New York, **1986**, and references cited therein.
[16] M. Yamanaka, A. Inagaki, E. Nakamura, *J. Comput. Chem.* **2003**, *24*, 1401–1409.
[17] a) K. Fukui, *Acc. Chem. Res.* **1981**, *14*, 363–368; b) C. Gonzalez, H. B. Schlegel, *J. Chem. Phys.* **1989**, *90*, 2154–2161; c) C. Gonzalez, H. B. Schlegel, *J. Phys. Chem.* **1990**, *94*, 5523–5527.
[18] a) R. McWeeny, *Phys. Rev.* **1962**, *126*, 1028–1034; b) R. Ditchfield, *Mol. Phys.* **1974**, *27*, 789–807; c) K. Wolinski, A. J. Sadlej, *Mol. Phys.* **1980**, *41*, 1419–1430; d) K. Wolinski, J. F. Hinton, P. Pulay, *J. Am. Chem. Soc.* **1990**, *112*, 8251–8260.
[19] a) J. Bigeleisen, M. G. Mayer, *J. Chem. Phys.* **1947**, *15*, 261–267; b) J. Bigeleisen, M. Wolfsberg, *Adv. Chem. Phys.* **1958**, *1*, 15–76.
[20] A. P. Scott, L. Radom, *J. Phys. Chem.* **1996**, *100*, 16502–16513.
[21] S. F. Boys in *Quantum Theory of Atoms, Molecules, and the Solid State* (Ed.: P. O. Lowdin), Academic Press, New York, **1968**, p. 253.
[22] M. Yamanaka, S. Kato, E. Nakamura, *J. Am. Chem. Soc.* **2004**, *126*, 6287–6293.
[23] a) A. E. Dorigo, J. Wanner, P. v. R. Schleyer, *Angew. Chem.* **1995**, *107*, 492–494; *Angew. Chem. Int. Ed. Engl.* **1995**, *34*, 476–478; b) J. P. Snyder, *J. Am. Chem. Soc.* **1995**, *117*, 11025–11026; c) E. Nakamura, M. Yamanaka, S. Mori, *J. Am. Chem. Soc.* **2000**, *122*, 1826–1827.
[24] For examples of related η^3-metal complexes, see: a) K. Tsutsumi, S. Ogoshi, S. Nishiguchi, H. Kurosawa, *J. Am. Chem. Soc.* **1998**, *120*, 1938–1939; b) S. Ogoshi, Y. Fukunishi, K. Tsutsumi, H. Kurosawa, *J. Chem. Soc. Chem. Commun.* **1995**, 2485–2486.
[25] a) E. Nakamura, M. Yamanaka, *J. Am. Chem. Soc.* **1999**, *121*, 8941–8942.; b) M. Yamanaka, E. Nakamura, *J. Am. Chem. Soc.* **2005**, *127*, 4697–4706.
[26] The 1,4- and 1,6-addition pathways via reductive elimination of **3c** at the C4 atom and of **5c** at the C6 atom require very high activation energies (>20 kcal mol^{-1}) and are thus omitted from Scheme 4. See Supporting Information for all the reaction pathways.
[27] Change of basis set from 321SDD to 6311SDD resulted in relative energy changes of 3–5 kcal mol^{-1}.
[28] L. Melander, W. H. Saunders, Jr., *Reaction Rates of Isotopic Molecules*, Wiley, New York, **1980**.
[29] D. A. Singleton, A. A. Thomas, *J. Am. Chem. Soc.* **1995**, *117*, 9357–9358.
[30] a) D. E. Frantz, D. A. Singleton, J. P. Snyder, *J. Am. Chem. Soc.* **1997**, *119*, 3383–3384; b) D. E. Frantz, D. A. Singleton, *J. Am. Chem. Soc.* **2000**, *122*, 3288–3295; c) N. Yoshikai, E. Nakamura, *J. Am. Chem. Soc.* **2004**, *126*, 12264–12265.
[31] Y. Yamamoto, S. Yamamoto, H. Yatagai, Y. Ishihara, K. Maruyama, *J. Org. Chem.* **1982**, *47*, 119–126.

Received: February 20, 2006
Published online: July 12, 2006

